

# Monterey Formation porcelanite reservoirs of the Elk Hills field, Kern County, California

S. A. Reid and J. L. McIntyre

## ABSTRACT

Oil and gas production from Monterey Formation porcelanite at the Elk Hills field in California's San Joaquin basin occurs from intervals that have quartz-phase mineralogy. However, characteristics differ from chert and porcelanite reservoirs of the coastal California Monterey Formation in that matrix porosity is more typical of the opal-CT phase, petroleum storage is mostly in the matrix, and natural fracture patterns are dominantly small scale. Several Elk Hills reservoirs located on two large anticlines produce from porcelanite. The 29R AB and 31S D are the most productive porcelanite reservoirs, each having cumulative oil production of about 40 million bbl. Although interbedded with siliceous shale, sandstone, and dolomite, most of the porous reservoir rock is laminated porcelanite. Porosity averages between 20 and 25% and is evenly distributed throughout the porcelanite as extremely small pores ranging in size from 1 to 10  $\mu\text{m}$ . Matrix permeability averages 0.8 md, but flow of oil and gas is enhanced through fractures parallel with and perpendicular to bedding. Higher than anticipated porosity may be in part due to migration of hydrocarbons into the porcelanite reservoirs while still in opal-CT-phase mineralogy. The dissolution of opal-CT and precipitation of quartz occurs in place, and the resulting quartz-phase mineral structure mimicks the porous opal-CT framework.

## INTRODUCTION

Significant oil and gas production occurs from Monterey Formation porcelanite reservoirs at the Elk Hills field in the San Joaquin basin of central California (Figure 1). Several wells in the 29R AB and 31S D reservoirs have produced in excess of one million bbl of oil, indicating the presence of significant reservoir storage and an effective permeability system, contrary to classic views of Monterey

## AUTHORS

S. A. REID ~ *Occidental of Elk Hills, Inc., P. O. Box 1001, Tupman, California, 93276; tony\_reid@oxy.com*

Stephen Anthony Reid is a senior geological advisor for Occidental of Elk Hills, Inc. He received his B.S. and M.S. degrees from California State University, Northridge. His work on the Miocene reservoirs of Elk Hills has focused on the identification of trapping characteristics of Stevens turbidite systems and on development of reservoir models for Monterey Formation porcelanite reservoirs.

J. L. MCINTYRE ~ *Occidental of Elk Hills, Inc., P. O. Box 1001, Tupman, California, 93276; jana\_mcintyre@oxy.com*

Jana McIntyre works as a development geologist for Occidental of Elk Hills, Inc. She has worked on several Miocene Monterey Formation turbidite and porcelanite reservoirs at Elk Hills and is currently working on shaly sandstone reservoirs of the Pliocene Etchegoin Formation. She received her geology degrees from the University of California at Davis (B.S.) and Oregon State University (M.S.).

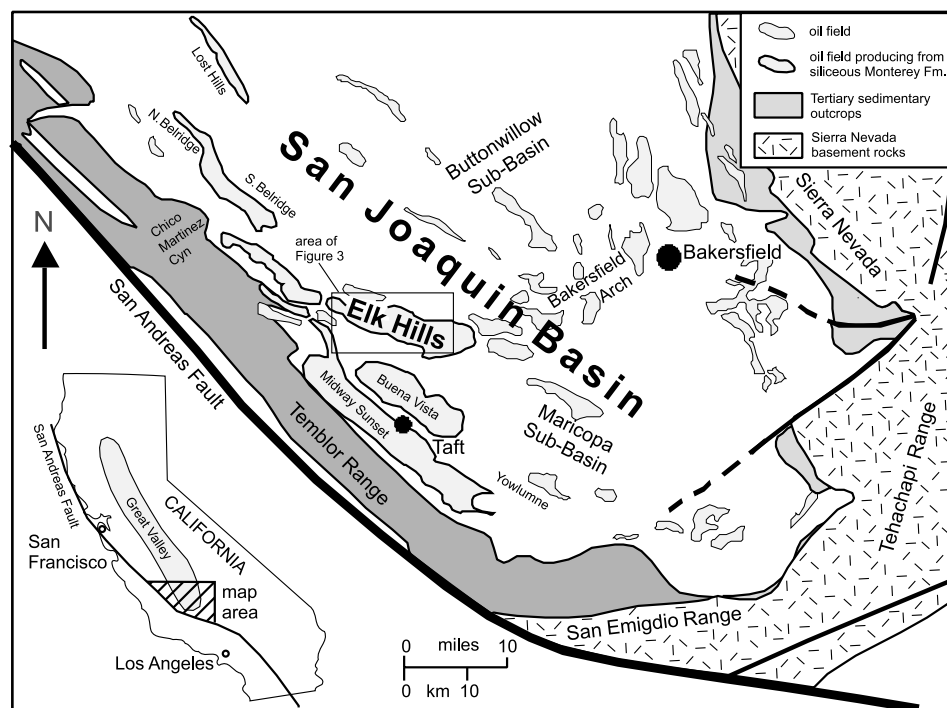
## ACKNOWLEDGEMENTS

We appreciate the contributions of the following individuals in preparing this reservoir model: Tor Nilsen for Monterey facies identification; JoAnn Conard for fracture descriptions; Drew Dickert, Greg Lord, and Bob Horton for observations on microscopic textures; and Tom Hampton for reservoir engineering comments. Jim Rogers, Mark Longman, Richard Behl, and Ray Sorenson provided helpful suggestions on improving the initial manuscript. We also thank the management of Occidental of Elk Hills, Inc., for permission to publish this article.

Copyright ©2001. The American Association of Petroleum Geologists. All rights reserved.

Manuscript received October 28, 1999; revised manuscript received March 14, 2000; final acceptance March 22, 2000.

**Figure 1.** Index map of the southern San Joaquin basin showing the location of the Elk Hills field and other large oil fields that produce from the siliceous facies of the Monterey Formation. Detailed geology of the Elk Hills area is shown in Figure 3.



siliceous shale as fracture-dominated reservoir systems. In fact, these Elk Hills reservoirs consist of a porous matrix produced through a system of fractures oriented parallel with and perpendicular to bedding. Porosity is unexpectedly high considering that the matrix is composed mostly of microcrystalline quartz. The origin of these unusual reservoirs is the result of the original depositional setting, early migration of hydrocarbons (before the final stage of silica diagenesis), and preservation of porosity as opal-CT dissolves and quartz precipitates.

Porcelanite is composed primarily of microcrystalline silica and, following the usage of Bramlette (1946), Murata and Larson (1975), Williams (1982), and Dholakia et al. (1998), is characterized by a subvitreous luster that resembles broken unglazed porcelain. Porcelanite of the Monterey Formation is the product of a diagenetic process that begins with deposits of siliceous diatom tests. The conversion from diatomite to quartz is well documented in the literature (i.e., Murata and Larson, 1975; Isaacs, 1981a; and Graham and Williams, 1985, among others). The process begins with tests of diatoms that consist of amorphous hydrated silica (opal-A phase). Deposits of high concentrations of diatoms, where lithified as diatomite, have an extremely high porosity (55–60%) (Isaacs, 1981b). With burial and increasing time, formation pressure, and temperature, the opal-A chemical structure be-

comes unstable and dissolves, yielding precipitation of a more stable mixture of cristobalite and tridymite (opal-CT phase) (Williams et al., 1985). The principle elements of opal-A (silica and oxygen) combine in a more tightly packed crystalline structure that has less surface area (Williams et al., 1985). Opal-CT-phase porosity decreases to 25–35% in the most silica-rich samples (Isaacs, 1981b). The opal-CT-phase mineralogy in turn becomes unstable over time, as the overburden thickness increases and formation pressure and temperature continue to rise. Cristobalite and tridymite dissolve, and more stable microcrystalline quartz precipitates (quartz phase) (Williams et al., 1985). In the coastal basins of California, chert and porcelanite can form as precipitating quartz fills much of the remaining porosity (resulting porosity averaging between 10 and 20%) (Isaacs, 1981b). The diagenetic process of converting opal-A to chert is accompanied by fluid flow due to dehydration reactions and chemical compaction (Eichhubl and Behl, 1998). The porosity reduction occurs as the matrix framework collapses and the rock compacts, and if the diagenetic water cannot be released, high pore fluid pressures may result in the formation of significant fracture networks, as observed in Monterey rocks in the coastal basins of California (Eichhubl and Boles, 1998).

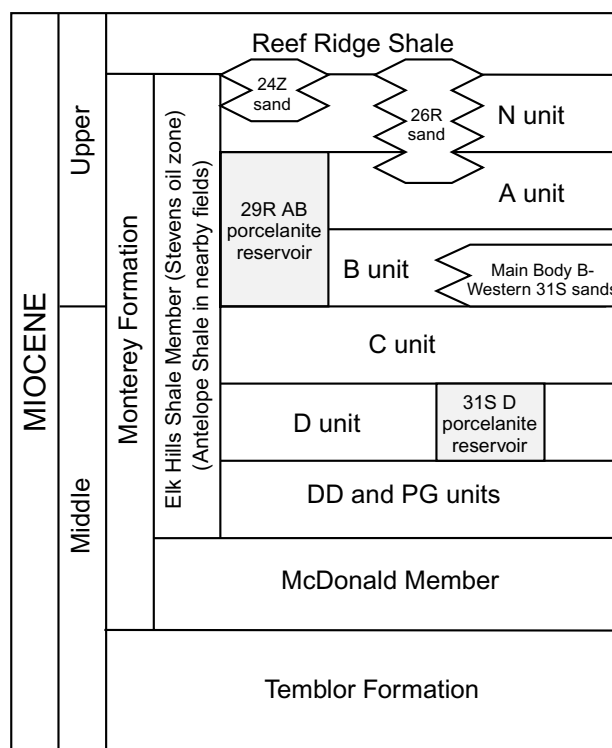
The formation of porcelanite at the Elk Hills area is believed to follow this diagenetic process, but the

resulting product differs in two major ways: (1) although clearly quartz phase, porosity is more characteristic of the opal-CT phase (measurements averaging between 20 and 25%), and (2) diagenetic-involved fracturing is minor, and few major fracture planes exhibit precipitation of silica; instead, most fracturing seems of tectonic origin. This article documents this unusual matrix character and presents a hypothesis regarding why the quartz-phase rocks at Elk Hills form a porous matrix similar to the opal-CT phase. We also discuss the impact of natural fractures in the formation of the porous porcelanite matrix.

## ELK HILLS OIL FIELD

The Elk Hills field, which has current cumulative oil production of more than 1.1 billion bbl (California Division of Oil and Gas, 1998), is located in the southwestern part of the San Joaquin basin, about 40 km (25 miles) southwest of Bakersfield, California (Figure 1). The field is named for hills that rise about 300 m (1000 ft) above the flat San Joaquin Valley floor, and the productive area extends more than 115 km<sup>2</sup> (45 mi<sup>2</sup>) along the crest of the hills. Although discovered in 1919, the field remained mostly shut-in until 1976 because of its designation as a naval petroleum reserve. The U.S. Department of Energy's interest in the field was acquired by Occidental Petroleum on February 5, 1998; Chevron U.S.A., Inc. also holds an interest in the field. Occidental of Elk Hills, Inc. serves as operator of the Elk Hills unit. During 1997, daily field production averaged 54,400 bbl of oil and 350 mmcf of gas from 1034 active producing wells (California Division of Oil and Gas, 1998).

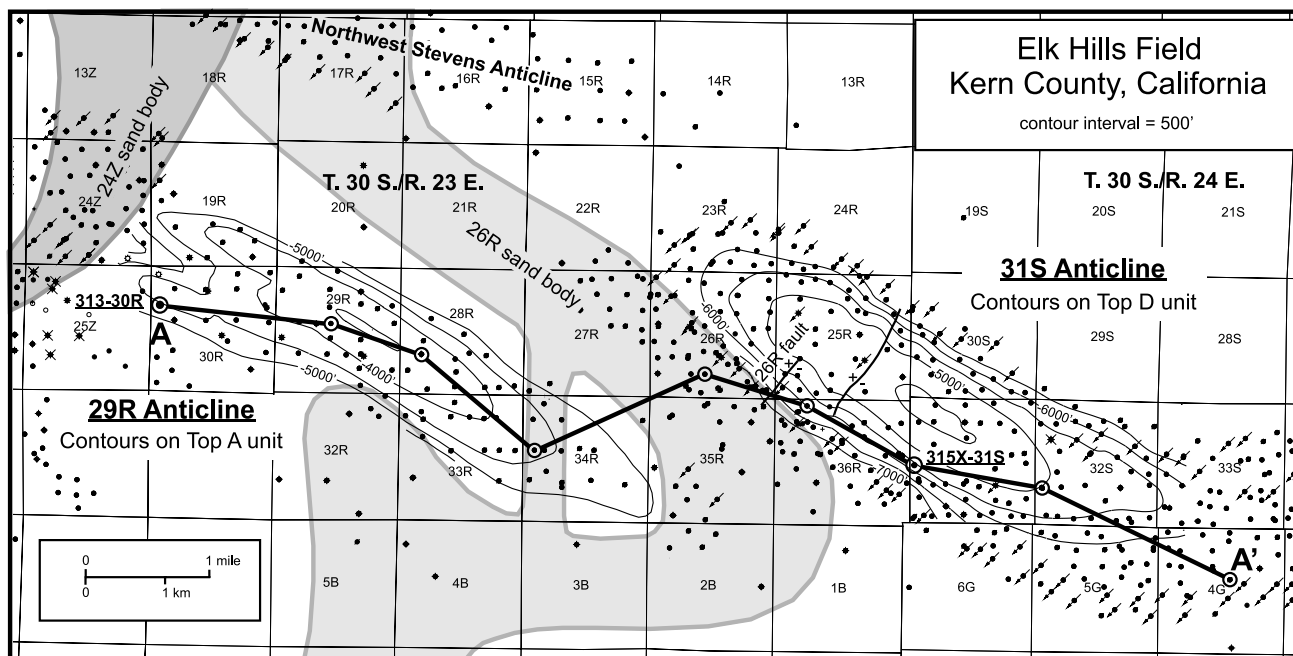
The porcelanite reservoirs of the Elk Hills field are within the Elk Hills shale member of the Miocene Monterey Formation (Maher et al., 1975). The Elk Hills shale member (a name not generally used beyond the limits of the field) correlates to the Antelope Shale Member, the name used more commonly in the basin (Dunwoody, 1986) (Figure 2). The porcelanite reservoirs are also within the Stevens oil zone, one of four petroleum-bearing zones in the field (Maher et al., 1975). In addition to the porcelanite reservoirs, the Stevens zone contains several major sandstone pools in structural and stratigraphic traps on three large anticlines. The Stevens is further divided into five producing units lettered (youngest to oldest) N, A, B, C, and D. Stevens pools range in depth from 1500 to 3000 m (5000 to 10,000 ft), and many wells are completed in



**Figure 2.** Stratigraphic column of the producing units of the Elk Hills shale member (Stevens oil zone), Monterey Formation, at Elk Hills and nearby fields (Maher et al., 1975). Significant porcelanite-producing units include the 29R AB and 31S D reservoirs.

oil columns originally 150 to 300 m (500 to 1000 ft) thick. Porcelanite reservoirs occur laterally adjacent to, overlying, and underlying sandstone reservoirs. All Stevens sandstone pools are of turbidite origin and are deposited in middle fan lobes (B unit) (Reid and Wilson, 1990) and as multistory sand bodies such as the 26R sand (N and A units of Figure 3) (Reid, 1990). Production from larger Stevens sandstone reservoirs is assisted through secondary recovery projects, including water flooding and gas injection for pressure maintenance. Porcelanite reservoirs are produced under primary recovery methods. Produced oil from all Stevens pools averages 35° API and has abundant associated produced gas.

At Elk Hills, porcelanite reservoirs occur on the 29R and 31S anticlines (Figures 3, 4). The northwest-trending 29R anticline is in the western half of Elk Hills and contains the N, AB, and D porcelanite reservoirs. The west-trending to northwest-trending 31S anticline is in the central and eastern parts of Elk Hills and contains the N and D porcelanite reservoirs, as well as



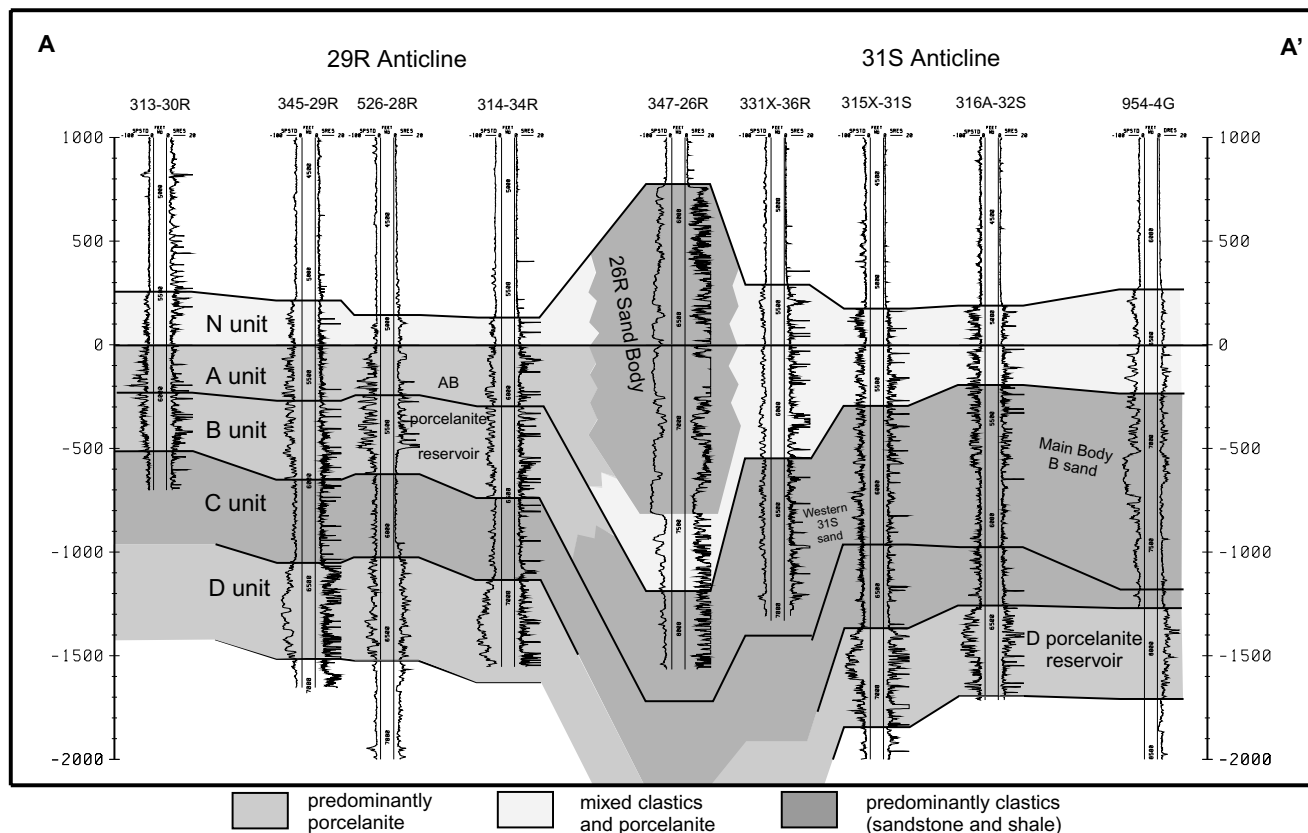
**Figure 3.** Structure maps of the 29R and 31S anticlines. Contours are on top A (west) and top D markers; contour interval is 500 ft. Key core wells used in this study are 313-30R and 315X-31S. Path of cross section AA' (Figure 4) is shown. Distribution of sand bodies present during deposition of the A and N units is from Reid (1990).

mixed porcelanite and sandstone reservoirs in the A and B intervals. Both anticlines are elongate domes that have steep limbs dipping to  $70^\circ$  and gently plunging fold noses. The only significant fault within the reservoirs is the 26R fault, a normal fault perpendicular to the fold axis of the 31S anticline. Structural growth has accelerated since the late Pliocene to form the petroleum traps on the current large anticlines (Maher et al., 1975), which have about 1800 m (6000 ft) of structural relief at the level of the N unit.

## DEPOSITIONAL SETTING

The Monterey Formation at Elk Hills is middle to late Miocene in age (Maher et al., 1975) and was deposited in a dynamic setting of evolving subsea structures in a deep-water setting (600–1200 m [2000–4000 ft]) (Bandy and Arnal, 1969). Deposition of the Monterey occurred after the development of the San Andreas fault and the transformation of the San Joaquin basin from a convergent to a transform margin setting (Graham et al., 1989). Wrench tectonism produced a complex sea floor similar in geomorphology to the current California borderland (Graham et al., 1982). By the late Miocene, several San Joaquin structures were ac-

tively growing, including those at Buena Vista Hills, Elk Hills, and Lost Hills (Harding, 1976). With removal of 265 km (150 mi) of post-Miocene offset on the San Andreas fault, the emergent Gabilan Range (Salinian high) lay west of the basin (Graham, 1978), resulting in partial closure of the west side of the basin. The deep marine setting within the basin became ideal for the preservation of organic-rich diatomaceous source rocks (Graham and Williams, 1985). Organic-rich shales collected in abundance in areas removed from coarse-grained deposition, including on the crests of the growing subsea anticlines (banktops). Banktop deposition of diatom debris in the Elk Hills area was less diluted by clastics and may indicate the growing anticlines were substantially above the basin floor. From the sides of the basin, sand-rich sediment derived from granitic highlands poured into the basin, creating Stevens submarine fans that prograded across the deep floor of the southern basin (MacPherson, 1978; Webb, 1981). At Elk Hills, periods of predominately diatom sedimentation were interrupted initially by the Kern River-derived Stevens fan system (during the B unit) and later by smaller westerly derived channel-like systems (during the A and N units) (Reid, 1990, 1995; Reid and Wilson, 1990). These smaller turbidite systems prograded northward to the basin floor, diverted



**Figure 4.** Stratigraphic cross section oriented from west to east across the 29R and 31S anticlines, Elk Hills field, showing the distribution of major sandstone units and porcelainite reservoirs. Cross section datum is at the top of the A unit. Stratigraphic thicknesses and measured depths are in feet. Log curves are SP (left) and resistivity.

by growing subsea anticlines (Reid, 1990). Periods of significant antinodal growth resulted in an abrupt segregation between turbidites and diatom debris, such as on the 29R anticline during B and A zone deposition (Figure 3). During periods of slower structural growth, a mixture of biogenetic siliceous material and clastics collected (for example, the N and A intervals on the 31S anticline).

## METHODS OF STUDY

Although developed and produced since 1976, relatively few cores of the porcelainite reservoirs have been studied in detail. Through initial development of the field, the geologic and producing characteristics of the porcelainite reservoirs were not fully understood. Efforts of the field's technical staff focused on developing petrophysical models, but most of these studies were incomplete because lithology, texture, and layering were not accurately described. As oil production de-

clined and water cut increased, a more detailed reservoir description of the porcelainite intervals was required to improve well performance. The focus of current studies on the most productive porcelainite reservoirs is to improve understanding of reservoir characteristics that control petroleum storage and movement, including (1) constructing a detailed model of the porcelainite matrix and proposing mechanisms for the origin of the unexpectedly high porosity, (2) describing the fracture orientation and density and their significance in the reservoir producing system, and (3) determining how oil and gas move from the porcelainite matrix into the wellbores.

To understand the productive mechanism of the Elk Hills porcelainite reservoirs, extensive core samples were obtained from two wells (313-30R and 315X-31S) (Figure 3). In addition to routine core analysis (porosity, air permeability, and fluid saturation), samples were analyzed for composition using bulk and clay x-ray diffraction analysis (Table 1). A shortcoming of bulk x-ray diffraction is that total clay

**Table 1.** Mineralogical Data from X-Ray Diffraction Analyses of Fine-Grained Lithologies (Bulk and Clay) (in wt. %)\*

Core Depth (in ft)	Quartz**	Opal-CT	Felds†	Calcite	Dolo‡	Siderite	Total Clay§	(I/S	I/M	Kaol	Chlor)	Pyrite	Other§§
<b>Chert/Porcelanite</b>													
Well 313-30R													
5820.3	93	—	4	tr	tr	—	1	tr	1	tr	—	2	—
5821.3	94	—	2	tr	—	1	1	tr	1	tr	—	2	—
5823.6	90	—	5	tr	tr	1	1	tr	1	—	—	2	1 <sup>N</sup>
5827.35	92	—	5	1	—	tr	1	—	1	—	—	2	tr <sup>N</sup>
5831.0	59	35	3	tr	—	—	1	tr	1	tr	—	1	1 <sup>N</sup>
5836.5	66	28	4	—	—	—	1	tr	1	—	—	1	—
5840.85	51	30	4	—	9	tr	5	3	2	—	—	1	1 <sup>M</sup>
5843.1	92	tr	3	tr	1	—	1	tr	1	—	—	2	1 <sup>N</sup>
5850.0	82	—	3	tr	10	—	1	tr	1	tr	—	4	—
5880.1	78	—	8	1	1	tr	5	2	3	tr	—	6	—
5882.9	69	22	5	1	tr	tr	1	tr	1	—	—	2	—
5883.45	88	—	5	1	tr	tr	2	tr	2	—	—	3	1 <sup>N</sup>
5905.1	95	—	2	tr	tr	—	1	tr	1	—	—	2	—
5917.8	92	—	2	2	1	—	1	tr	1	—	—	2	—
5919.0	91	—	5	1	tr	1	1	tr	1	tr	—	1	tr <sup>M</sup>
5937.75	93	—	3	tr	1	1	1	—	1	—	—	1	tr <sup>M</sup>
5941.45	82	—	5	1	10	tr	1	tr	1	tr	—	1	—
5944.0	78	—	9	—	—	—	10	2	4	4	tr	1	—
5955.8	92	—	5	—	tr	—	2	tr	2	tr	—	1	—
5956.45	70	22	6	tr	—	—	1	tr	1	—	—	1	—
5978.1	89	tr	5	2	1	tr	1	tr	1	—	—	2	—
5999.7	91	—	5	1	1	tr	1	tr	1	tr	—	1	tr <sup>M</sup>
6004.7	91	—	3	2	1	tr	1	tr	1	tr	—	1	—
6019.7	92	—	4	—	—	—	2	tr	1	1	—	2	—
6042.0	84	—	7	3	tr	1	3	1	2	tr	—	2	—
6047.2	92	—	3	2	1	tr	1	tr	1	tr	—	1	tr <sup>N</sup>
6054.3	74	—	3	1	19	tr	2	tr	1	1	—	1	—
6072.0	91	—	2	5	—	—	1	tr	1	—	—	1	—
6076.6	68	13	13	2	—	—	1	tr	1	tr	—	3	—
6089.7	94	—	2	1	1	tr	1	—	1	—	—	1	—
6090.5	86	—	4	5	1	1	2	tr	1	1	—	2	—
6096.95	85	—	7	tr	1	—	4	1	2	1	—	3	—
6106.2	95	—	2	—	tr	tr	1	tr	1	—	—	2	—
6114.85	93	0.4	3	—	—	—	1	0.2	1	0.4	—	2	—
6120.6	95	—	2	—	1	—	1	tr	1	—	—	1	—
6126.58	90	—	2	5	tr	—	1	tr	1	tr	—	2	—
6143.6	95	—	2	1	—	tr	1	tr	1	tr	—	1	—
6167.2	86	—	2	—	10	—	2	—	1	1	—	1	—
6179.9	93	—	3	1	tr	—	1	tr	1	tr	—	2	—

*continued*

may be underestimated owing to poor detection of particles less than 10  $\mu\text{m}$  in size (Ruessink and Harville, 1992). To provide additional information on de-

trital components (including quartz grains), thin sections were prepared for selected samples and point counted to determine composition. To more accu-

**Table 1.** Continued

Core Depth (in ft)	Quartz**	Opal-CT	Felds†	Calcite	Dolo‡	Siderite	Total Clay§	(I/S	I/M	Kaol	Chlor)	Pyrite	Other§§
<b>Well 315X-31S</b>													
6722.2	83	—	5	9	1	—	1	0.3	0.7	—	—	1	—
6724.15	70	—	9	8	1	1	tr	tr	—	—	—	11	—
6724.55	88	—	1	10	—	—	—	—	—	—	—	1	—
6724.95	81	—	7	6	2	—	2	—	2	—	—	2	—
6725.7	88	—	3	6	1	—	1	0.1	0.9	—	—	1	—
6755.3	88	—	4	4	1	—	1	—	1	—	—	2	—
6757.7	84	—	5	7	1	—	1	0.2	0.8	—	—	2	—
6766.3	83	—	6	6	1	—	2	0.1	1.9	—	—	2	—
6768.0	90	—	7	4	2	—	—	—	—	—	—	1	—
6782.6	90	—	1	5	2	—	1	1	—	—	—	1	—
6784.1	80	—	3	9	7	—	tr	tr	—	—	—	1	—
6786.5	91	—	3	4	1	—	tr	tr	—	—	—	1	—
6795.9	90	—	3	5	1	—	tr	tr	—	—	—	1	—
6807.1	84	—	7	5	1	—	2	0.3	1.7	—	—	1	—
6810.84	94	—	2	2	1	—	tr	tr	tr	—	—	1	—
6816.2	96	—	1	2	0	—	—	—	—	—	—	1	—
6816.4	98	—	—	1	—	—	—	—	—	—	—	1	—
6819.8	94	—	1	2	1	—	tr	—	tr	—	—	2	—
6831.95	97	—	—	2	—	—	—	—	—	—	—	1	—
6833.0	84	—	10	3	1	—	tr	tr	tr	—	—	2	—
6835.2	78	—	10	2	2	1	4	0.6	3.4	—	—	3	—
7026.95	88	—	4	2	4	1	tr	tr	—	tr	—	1	—
7028.1	81	—	7	3	5	2	1	0.4	0.4	0.2	—	1	—
7038.0	91	—	2	1	1	2	1	0.4	0.4	0.2	—	2	—
7047.0	93	—	2	1	1	1	tr	—	—	tr	—	2	—
7069.85	75	—	17	—	1	—	5	1	4	—	—	2	—
<b>High Detritus Porcelanite/Siliceous Shale</b>													
<b>Well 313-30R</b>													
5837.15	61	—	20	—	—	—	12	3	7	2	—	7	—
5838.2	24	1	11	—	—	—	61	38	2	21	—	2	—
5878.5	65	—	15	1	—	—	13	3	9	1	tr	6	—
5903.0	72	—	15	—	—	—	9	3	5	1	tr	4	—
6067.7	66	—	17	3	1	tr	10	4	5	1	—	3	—
<b>Claystone</b>													
<b>Well 313-30R</b>													
5823.05	5	—	42	—	—	—	31	23	1	7	—	20	—
6073.8	10	—	19	—	—	—	40	34	3	3	—	3	29 <sup>C</sup>
6155.35	4	—	19	2	—	2	23	13	3	7	tr	34	16 <sup>M</sup>

*continued*

rately describe the microporous matrix, scanning electron microscopy and confocal microscopy were used. Confocal microscopy is a relatively new technique that was developed for the biological sciences and is proving to be a valuable tool in the geosciences, as

well. This method allows high resolution imaging of thin sections (to 1  $\mu\text{m}$ ) for micropore size and geometry, as well as differentiation of macroporosity (fracture, intraparticle, and moldic) from interparticle microporosity (Fredrich et al., 1993).

**Table 1.** Continued

Core Depth (in ft)	Quartz**	Opal-CT	Felds <sup>†</sup>	Calcite	Dolo <sup>‡</sup>	Siderite	Total Clay <sup>§</sup>	(I/S	I/M	Kaol	Chlor)	Pyrite	Other <sup>§§</sup>
<b>Dolomite</b>													
<b>Well 313-30R</b>													
5851.15	19	tr	3	—	76	—	1	tr	1	—	—	1	—
5900.65	8	—	1	—	90	—	tr	—	tr	tr	—	1	—
5957.9	13	1	tr	—	86	—	tr	—	—	—	—	tr	—
5984.3	21	—	2	—	71	—	1	—	1	tr	—	5	—
6024.95	20	—	tr	—	78	tr	1	—	1	tr	—	1	—
6025.3	6	tr	—	—	93	—	1	—	1	—	—	—	—
6057.9	22	—	2	2	72	tr	1	tr	1	tr	—	1	—
6102.75	21	—	1	—	75	—	2	—	1	1	—	1	—
6104.1	6	—	tr	—	94	—	tr	—	—	—	—	tr	—
6118.3	8	—	tr	—	92	—	tr	—	tr	—	—	tr	—
<b>Well 315X-31S</b>													
6770.9	33	—	—	—	65	—	tr	tr	—	tr	—	2	—
6771.4	24	—	—	—	74	—	tr	—	—	tr	—	2	—
6814.0	8	—	—	—	92	—	tr	tr	—	—	—	—	—

\*Data from columns two to eight were normalized then plotted on the ternary diagram in Figure 6.

\*\*Detrital quartz included (typically ≤3% from petrography)

<sup>†</sup>Includes potassium and plagioclase feldspars

<sup>‡</sup>Includes dolomite, ferroan dolomite, and possibly minor ankerite or manganese dolomite

<sup>§</sup>I/S = 100% mixed layer illite/smectite in 313-30R; 100% smectite in 315X-31S; I/M = illite and muscovite

<sup>§§</sup>N = natrolite; M = marcasite; C = clinoptilolite (a zeolite)

## PORCELANITE RESERVOIRS

Although there are several porcelaneous intervals that produce in the Stevens oil zone, the 29R AB units and the 31S D unit are the most productive. The 29R AB reservoir covers about 9 km<sup>2</sup> (2550 ac) on the crest of the structure (Figure 3). The average gross pay thickness is about 150 m (500 ft), and the original oil-water contact is between 1585 and 1615 m (5200 and 5300 ft) subsea. Twenty-four active wells (on 15 to 20 ac spacing) produce at a daily rate (as of August, 1996) of 530/6300/8.0 (bbl of oil/bbl of water/mmc of gas) from this reservoir. Oil production declines at 8% per year, and the gas-oil ratio (GOR) is constant at 15,200 standard cubic ft (scf)/stock tank bbl (stb). The pool has been under active production since 1976, and cumulative production for most wells averages between 300,000 and 750,000 bbl of oil. The production mechanism is solution-gas drive augmented by moderate water influx, which helps keep the reservoir pressure nearly stable at about 1600 psi. The entire 29R reservoir (including associated sandstone pools in the N and A units and the D unit porcelanite) has produced about 40 million bbl of oil, or about 17% of the original oil

in place (U.S. Department of Energy, 1997a). By re-completing idle wells and drilling new wells, the porcelaneous intervals of the AB units are capable of producing up to an additional 9.5 million bbl of oil and 70 bcf of gas (U.S. Department of Energy, 1997a).

Most 31S D unit wells are produced along with the overlying C unit, which consists of thin beds of fine sandstone and siltstone that are probably of distal submarine fan origin. However, production logs and tests indicate most of the historic production is from the D interval. Production is from 11 km<sup>2</sup> (2700 ac) on the west end of the 31S anticline (Figure 3). Gross pay thickness averages about 150 m (500 ft), and the original oil-water contact (based on the results of well production tests) is at about 1830 m (6000 ft) subsea. A large secondary gas cap has formed above about 1700 m (5600 ft) subsea, leaving production restricted to a single row of wells in a narrow band on the north and south flanks of the structure. Recent daily production (August, 1996) is about 3000/7000/60.0 (bbl of oil/bbl of water/mmc of gas) from 55 active wells (10 to 20 ac spacing). Current reservoir pressure is at about 2000 psi. Natural drive mechanisms include gravity drainage, solution-gas drive, and water and gas influx.



These are augmented by gas leakage from the 26R reservoir along a fault and gas injection cycling from 1996 to 1998 for natural gas liquids (NGL) recovery. Cumulative oil production from most wells located on the north and south limbs of the 31S anticline ranges between 300,000 and 1,000,000 bbl, indicating that gravity drainage assists production. Total cumulative production from the CD units is about 38 million bbl of oil, or about 12% of the original oil in place (U.S. Department of Energy, 1997b). Expected remaining reserves from existing wells and infill drilling are as much as 20 million bbl of oil and 85 bcf of gas (U.S. Department of Energy, 1997b).

Production techniques for both reservoirs included cementing casing across the productive intervals and selectively perforating to avoid water-bearing, highly permeable, naturally fractured dolomite beds. Wells require acid stimulation using an HCl-HF mixture to clean up formation damage caused by drilling, cementing, and perforating. Most wells initially flow but require artificial lift after a few months. Wells drilled in 1995 initially produced 200–300 BOPD and stabilized over an 18-month period to 50–75 BOPD.

## LITHOLOGY OF RESERVOIR INTERVALS

### Distribution of Rock Types

Porcelanite reservoirs contain predominately porcelanite beds, as well as other rock types including dolomite, siliceous shale, siltstone, and sandstone (Figure 5). Clay-rich deposits are uncommon. The principal reservoir rock is low-detritus quartz-phase porcelanite, which contains less than 25% combined detritus and carbonate (Figure 6). Opal-CT porcelanite beds are present in a few intervals in core from well 313-30R and are more common on the structural crest of the 29R anticline, where the transition to quartz phase is not complete. Also present are debris flow and slump deposits that are composed of the same reservoir rock types. These associated lithologies interact with the porcelaneous intervals in controlling production by acting as barriers or conduits for fluid flow.

The 29R AB stratigraphic section consists of about 60% porcelanite beds and 30% interbedded siliceous shale beds and, less commonly, clay shale beds (Figure 5). A few beds of sandstone comprise about 5% of the total AB interval. Distinctive beds of dolomite also occur throughout the section at intervals

9–24 m (30–80 ft) apart and make up about 5% of the unit. The 31S D stratigraphic section also contains about 60% porcelaneous beds but has much less interbedded siliceous shale (only 5% of the unit). Much of the lower D section contains an interbedded mixture of porcelanite, mudstone, sandstone, siltstone, and thin dolomite beds (15% of the D). Slumps and debris flows are common (20% of interval) in laterally discontinuous intervals up to 30 m (100 ft) thick (Wilson et al., 1997).

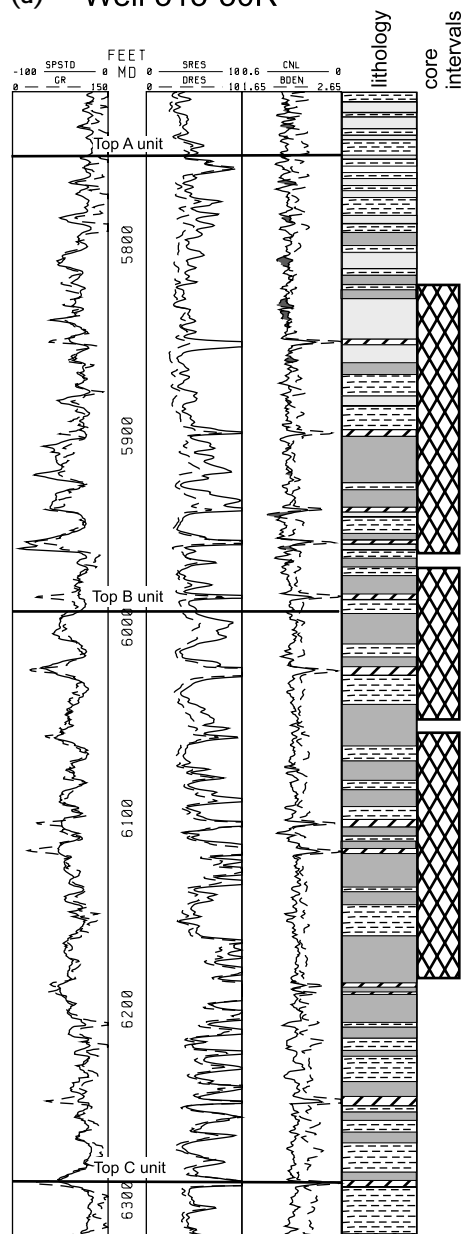
### High-Detritus Porcelanite, Siliceous Shale, and Mudstone

Oil-bearing porcelanite beds are interbedded and interlaminated with relatively clay-rich, nonreservoir rocks that are hard, medium gray-brown to dark gray, and have minor or no fluorescence. These nonreservoir rocks are comprised of high-detritus porcelanites, siliceous shales, and, uncommonly, soft, gray-black mudstone. High-detritus porcelanite is defined here as having x-ray diffraction concentrations of greater than 25% combined clastics and carbonates (Figure 6, Table 1). High-detritus porcelanite is a poor reservoir rock because clay isolates pores, resulting in permeabilities lower than for low-detritus porcelanite. These rocks are expected to contribute some gas, especially through desorption from organic material as reservoir pressure declines (McIntyre et al., 1997). High-detritus porcelanite and siliceous shale contain natural fractures but at lower intensities than in better reservoir quality porcelanites.

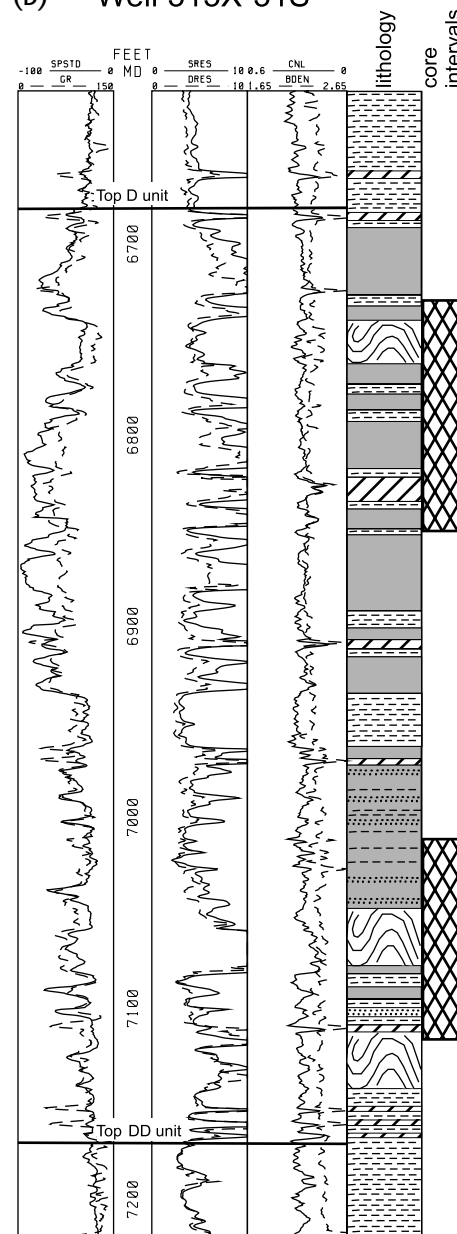
### Dolomite




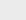
Dolomite interbeds are typically 0.3–1.5 m (1–5 ft) thick and occur within all porcelanite reservoirs at Elk Hills. Dolomitic layers are massive to laminated, commonly having gradational bed boundaries. Based on x-ray diffraction analyses, the carbonate beds contain 70–95% dolomite or ferroan dolomite, minor amounts of quartz, and traces of pyrite, feldspar, organic material, and clay. Dolomite is an early diagenetic product that is found forming in Holocene sediments off the Baja California coast within 40 cm of the sea floor at water depths greater than 1800 m (6000 ft) (Shimmield and Price, 1984). Samples that are less dolomitized (71–76 wt. % dolomite and 19–22 wt. % quartz) retain higher matrix porosities (13–32%). More complete dolomitization (samples having 86–94 wt. % dolomite and 6–13 wt. % quartz) typically results in lower matrix porosity and permeability but higher fracture intensity.

(a) Well 313-30R

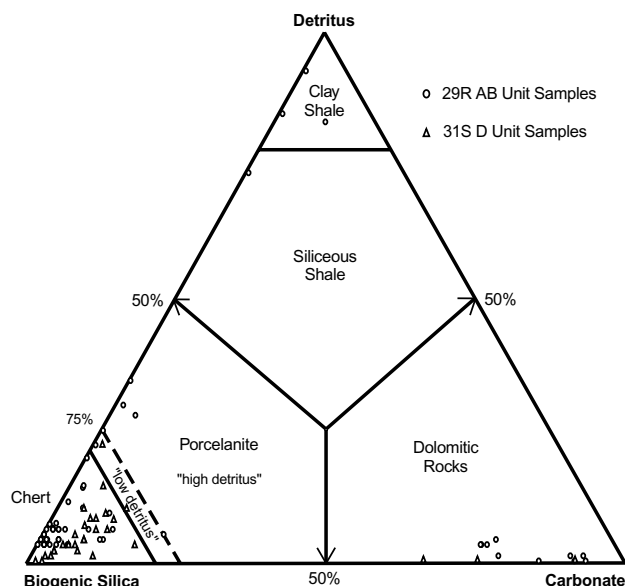


(b) Well 315X-31S



-  porcelanite (quartz phase)
-  porcelanite (mixed CT & quartz phases)
-  dolomite
-  debris flows and slumps

- Monterey Formation Porcelanite Reservoirs



**Figure 6.** Ternary diagram of silica, carbonate, and detritus composition of fine-grained Stevens oil zone intervals, based on x-ray diffraction analysis of samples from Table 1 (columns two through eight) for wells 313-30R and 315X-31S. Biogenic silica consists of quartz and opal-CT (columns two and three). Detritus is feldspars and total clay (columns four and eight). Carbonate is calcite, dolomite, and siderite (columns five, six, and seven). Samples typically fall into the chert part of the diagram, although textural characteristics are similar to porcelanite. Correction of data for detrital quartz content would shift the data only slightly toward porcelanite. Classification system after Williams (1982).

Where highly fractured, the dolomite beds are the most effective conduits for fluid movement.

## Sandstone

Although not common, beds of sandstone occur in the 29R AB and lower 31S D reservoirs. Individual beds range in thickness from 3 to 30 cm (0.1 to 1 ft) and are present as isolated beds or packages of beds up to 3 m (10 ft) thick (Figure 5). The sandstone is graded and laminated, medium to very fine grained, and moderately well sorted (clean laminations) to poorly sorted (clayey laminations). The sandstone beds are generally of poor reservoir quality because of chert cement that fills the pore space. These sandstones are probably turbidites, and commonly extend across the entire reservoir. The occurrence of sandstone in the 29R AB unit is not surprising given the significant turbidite sand bodies that exist nearby in laterally equivalent areas (26R sand and Main Body B sand, see Figure 4).

## Slumps

Lens-shaped slump deposits locally account for 20% of the D reservoir thickness on the 31S structure (Figure 5). In the upper D interval in well 315X-31S, slumps are composed of contorted beds of sand, silt, and mud of contrasting composition to the porcelaneous intervals above and below, suggesting a significant transportation from near a shelf area. Upper D slumps can be up to 30 m (100 ft) thick and cover nearly a square mile (Wilson et al., 1997). Slumps are considered poor reservoir rocks because of their interior heterogeneity and most likely act as barriers to fluid movement within the porcelaneous intervals.

## Porcelanite Composition

Most petroleum production from the 29R AB and 31S D reservoirs is from porcelanite beds. Based on x-ray diffraction analyses, porcelanite is composed of quartz (77–98 wt. %) (Table 1), feldspar (0–13 wt. %), clay (0–10 wt. %), carbonate cement (up to 19 wt. %), and nonclay cements including siderite and pyrite (up to 11 wt. %). Based on thin section modal analysis, only minor detrital quartz is present in the low-detritus porcelanite. Average detrital quartz concentration is 2% and not more than 6% in 18 sections analyzed. Organic material is amorphous kerogen, which is 1–7 wt. % of the rock, and, at the depth of the Elk Hills reservoirs, is not a mature source of petroleum. Clay consists of illite, illite/smectite, and kaolinite. X-ray diffraction indicates that some of the A unit porcelanite beds in well 313-30R have opal-CT mixed with quartz-phase chert (Table 1). A distinctive density shift on open-hole logs suggests that higher percentages of opal-CT-phase rocks may be present at shallower depths.

Using the mineralogical classification systems of Williams (1982) and Isaacs (1981c), most samples are classified as chert (greater than 80% quartz), although their texture and porosity are that of porcelanite (Figure 6). These rocks lack the vitreous luster and conchoidal fracturing of prototypical cherts, such as the more brittle Monterey Formation cherts from the coastal basins of California (as described by Isaacs [1981c]). Therefore, to prevent confusion with textural cherts, the reservoir rocks at Elk Hills are primarily referred to by their textural rock name of “porcelanite” (Williams, 1982), which typically has a dull luster similar in appearance to broken porcelain.

## MACROSCOPIC APPEARANCE OF RESERVOIR INTERVALS

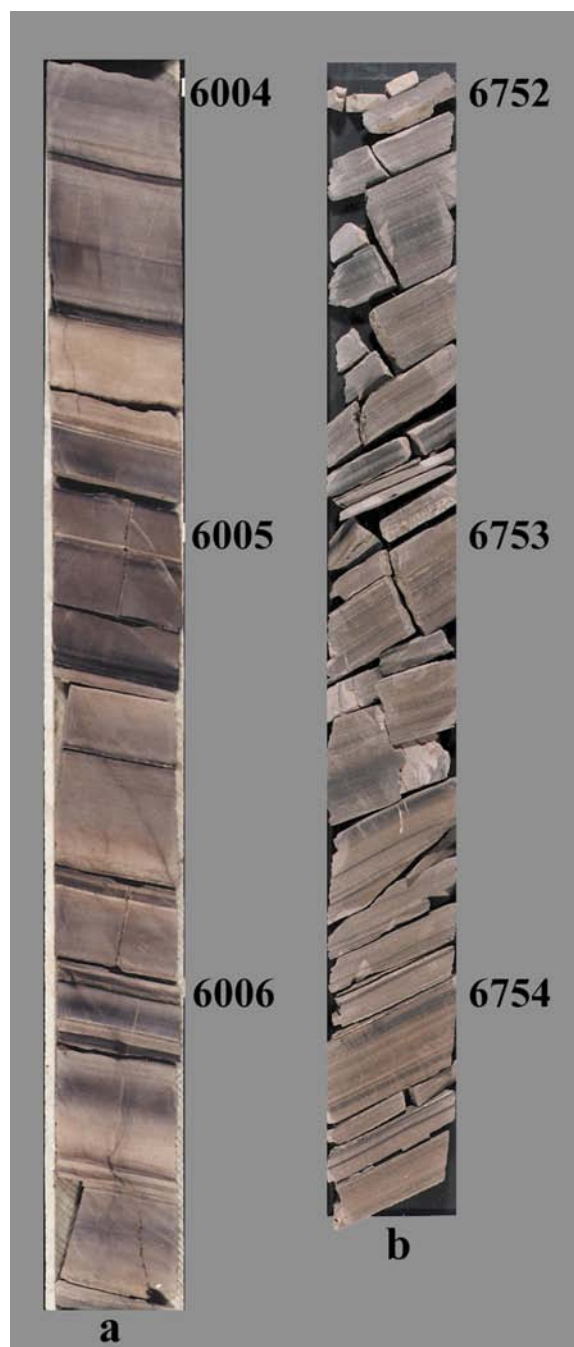
### Characteristics of Bedding

The productive reservoir intervals consist of hard, tan to medium gray-brown, dull to subvitreous, oil-bearing porcelanite interlaminated and interbedded with darker, clay-bearing and organic-bearing high-detritus porcelanite and minor beds of dolomite, claystone, and clastics (Figure 7). Under ultraviolet light, porcelanite has an even, moderate to bright yellow fluorescence reflecting significant oil saturations. Porcelanite differs from interbedded siliceous shale by having a lower specific gravity (owing to the high porosity), which is readily apparent in cores. Beds are typically 2–15 cm thick, and laminae are a few millimeters to a centimeter thick. A few cored porcelanite beds contain 22–35 wt. % opal-CT (mixed with quartz-phase silica) (Table 1) and are distinctive from primarily quartz-phase porcelanite in that their luster is always dull, fluorescence is absent or faint dull brown, and specific gravity is lower. Water sprayed on a slabbed surface of these core samples is quickly imbibed.

### Fractures

Natural fractures in the cores of the porcelanite reservoirs from wells 313-30R and 315X-31S fall into four categories: (1) larger fractures subperpendicular to bedding, (2) smaller fractures subperpendicular to bedding (Figure 7a), (3) fractures parallel with bedding (Figure 7b), and (4) healed fractures probably associated with initial compaction.

1. Large fractures are at least a meter long in core and are subperpendicular to bedding. Imaging logs indicate that large-scale fractures are longer and more common than can be directly inferred from core. Large fractures are characterized by relatively planar breaks in core, and noncalcitic mineralization on fracture surfaces is common. Large fractures occur in about half the cored section in the 29R AB reservoir and in only the lower part of the 31S D reservoir. Orientation of large fractures is parallel with wellbore breakouts observed at Elk Hills, which is the result of regional compressive stresses (Castillo and Zoback, 1994). Although larger fractures probably contribute to fluid production, well tests in well 313-30R indicate that intervals without identifiable large fractures are also oil productive.



**Figure 7.** Examples of typical porcelanite core, Elk Hills field. (a) Low-detritus oil-stained porcelanite (brown) interbedded with high-detritus porcelanite (light gray) and siliceous shale (dark gray) from well 313-30R, 29R AB reservoir. Small bed-perpendicular fractures are probably natural and contain silica, detritus, organic material, and oil staining. (b) Laminated low-detritus porcelanite finely interbedded with high-detritus porcelanite from well 315X-31S, 31S D reservoir. Numerous bedding-plane breaks at lithology changes are likely drilling induced. However, the structural model of Dholakia et al. (1998) would indicate that bedding-plane fractures should occur in areas of higher dip. Oil staining on some bedding breaks may support their model.



2. Small fractures have a planar shape and are generally subperpendicular to bedding (Figure 7a). They are commonly less than 0.3 m (1 ft) in length and commonly terminate at bedding contacts. Small fractures are primarily confined to low-detritus porcelanite and dolomite and are present in about half of the cored intervals. Small fractures are typically filled with silica, detritus, or organic material but are open in cores in about 5% of the occurrences.
3. Bedding-plane fractures are suspected to be important to the productivity of these reservoirs, especially on flanks of the structures (Figure 3). Breaks parallel with bedding surfaces commonly occur at bed boundaries containing organic material and clays. Evidence of natural open fractures is uncommon and includes visible porosity on unbroken core and unidentified noncalcareous fracture-filling mineralization. In areas of high dip (greater than 45°, as in the 31S D reservoir core in well 315X-31S), porcelanite intervals commonly contain 36 to 60 breaks parallel with bedding per meter (Figure 7b). In contrast, bedding-parallel breaks in the lower dip 29R AB reservoir core of well 313-30R generally average between 15 and 24 breaks per meter. Drilling and coring activities are probably responsible for some of the bedding fractures. However, during recovery of porcelanite cores, oil and gas commonly bubble through the encasing mud sheath along bedding planes, and free oil is present along some of the

broken bedding-plane surfaces. Oil and gas shows provide direct evidence that bedding-plane fractures may be present and common in the subsurface.

4. Healed fractures form irregular, anastomosing traces pervasive in the upper A unit core from well 313-30R and occur at a rate of up to 18 per meter in the B unit. These features are commonly present in subparallel sets at high angles to bedding and are less than 3 cm high. They are commonly filled with clay or kerogen and uncommonly act as conduits. These fractures are the earliest breaks to occur. Grimm and Orange (1997) describe similar fractures as occurring shortly after burial on tectonically unstable slopes. This origin is consistent with the slump features in the 31S D reservoir and the anticline growth associated with the 29R AB reservoir.

## MICROSCOPIC APPEARANCE

Thin sections demonstrate that porous low-detritus porcelanite can be very finely laminated with wavy, dark brown, organic and clay-rich layers, as well as containing some laminae of very fine sandstone, siltstone, or carbonate (Figure 8). Porcelanite commonly has a blue tint in thin section, which is due to the blue epoxy used in thin-section preparation that fills the abundant



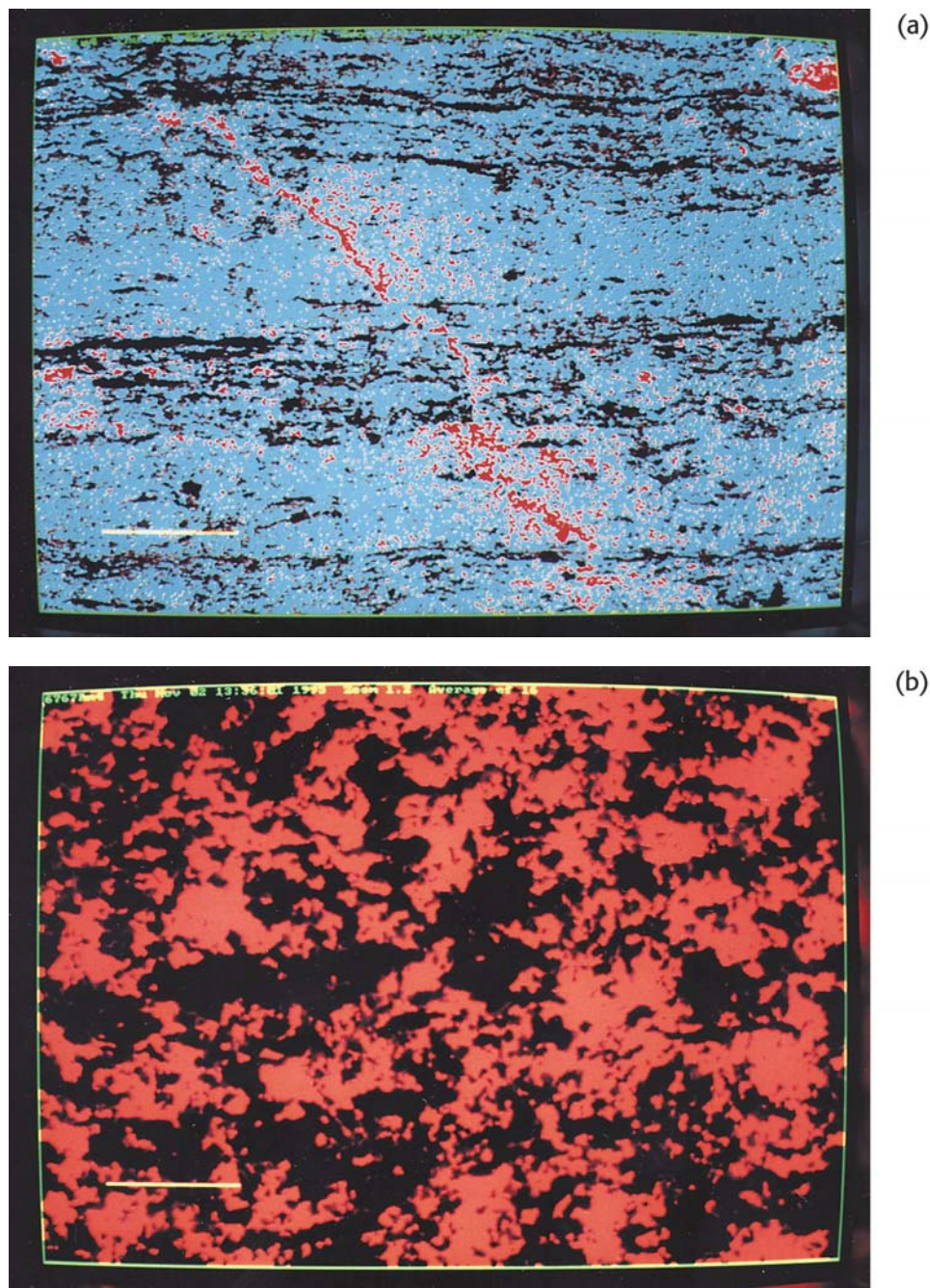
**Figure 8.** Photomicrograph of sample from 6811.6 ft (2076 m) in well 315X-31S (31S D unit) showing typical characteristics of laminated silty porcelanite. Intervals having a blue tint are porcelanite laminae, and colored epoxy indicates the microporous matrix. Laminae having higher clay and organic material content are darker. Molds of fossil fragments (upper and lower edges) average 0.125 mm in diameter. Diameter of photomicrograph is 4.0 mm.



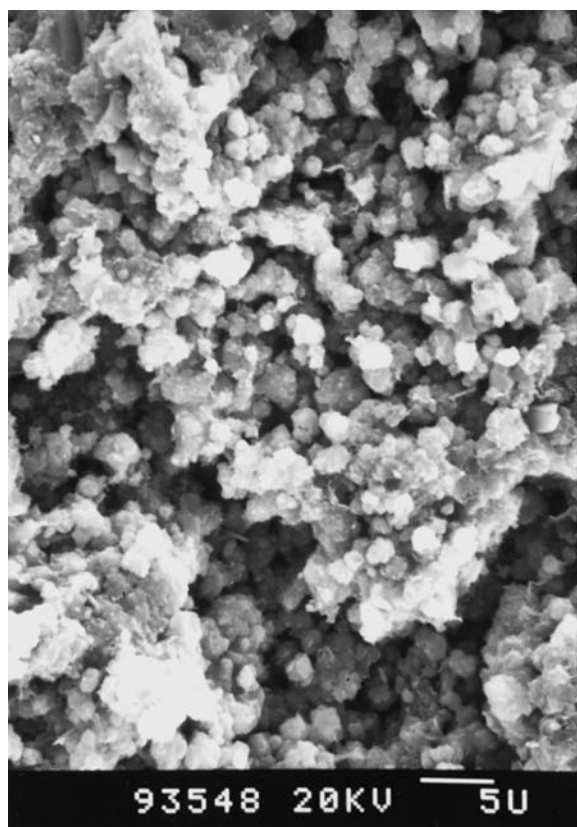
microporous matrix. Foraminifera and unaltered diatom remnants are common.

From thin section point counts, porosity appears low, from 2 to 12%, reflecting the difficulty of resolving microporosity in a standard thin section. Thin sections do provide a relative porosity perspective between porous, bluish porcelainite laminae and darker, organic-rich laminae that have generally low porosity. Routine core analyses yield porosities generally between 20 and 27% but ranging from 15 to 42%. Beds

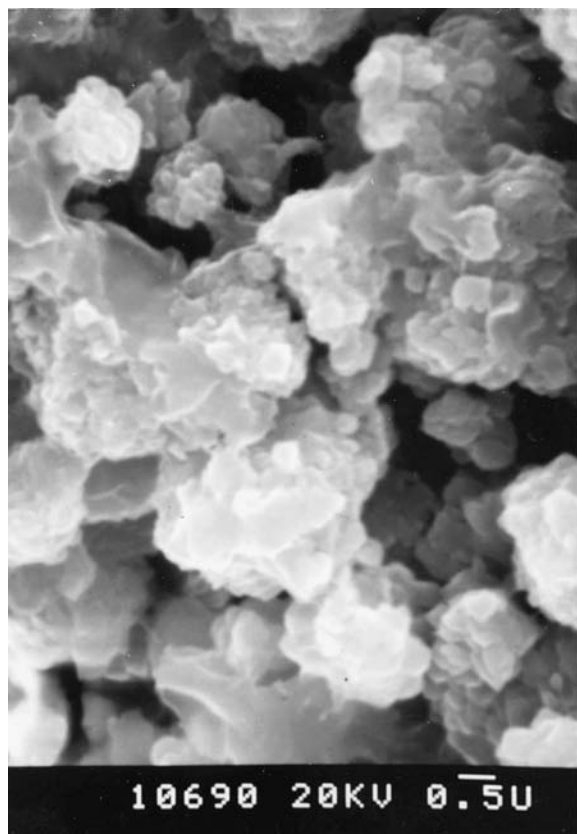
having mixed quartz and opal-CT (22–35 wt. % opal-CT) have slightly higher core porosities, averaging 33% and ranging from 27 to 45%. Confocal microscopy porosity estimates are similar to the core analyses, having individual measurements between 20 and 31%. Owing to this method's superior ability to resolve microporosity, these values are probably the most accurate (Figure 9). In many samples, porosity is shown to be evenly disseminated through the sample. Average pore diameter is 10  $\mu\text{m}$ . Scanning elec-



**Figure 9.** Confocal microscopy images of porcelainite from 6767.8 ft (2062 m) in well 315X-31S (31S D unit) having a calculated porosity of 19%. (a) At low magnification, laminations of nonporous matrix (black) alternate with porous porcelainite (mixed microporosity and quartz; blue). An open fracture (center) exhibits macroporosity (red). Scale bar at lower left is 500  $\mu\text{m}$ . (b) Porcelainite at high magnification contains a faintly laminated nonporous quartz matrix (black) and interconnected microporosity (red). Scale bar at lower left is 25  $\mu\text{m}$ .



(a)



(b)

tron microscope photomicrographs also illustrate the microporous nature of the porcelanite (Figure 10) that has pores as small as 1  $\mu\text{m}$  in diameter. In less porous areas, euhedral microcrystalline quartz occurs as more thickly intergrown masses. Confocal microscopy illustrates the low permeability and reduced storage capacity of high-detritus porcelanite interbeds that contain more isolated microporous patches and low total porosities (Figure 11). Wire-line log porosity most closely matches the core analysis and confocal estimates.

Microfractures are generally confined to the porcelanite intervals and are both parallel with bedding and at a high angle (subperpendicular) to bedding. Fractures parallel with bedding occur mostly at bed boundaries and between quartz-rich and organic-rich laminations (Figure 12). No direct petrographic evidence exists to confirm that these fractures are natural, and most may be a product of drilling damage or the thin-section manufacturing process. Nonetheless, oil-bearing bedding planes on fresh core would suggest that open fractures might exist at the microscopic scale.

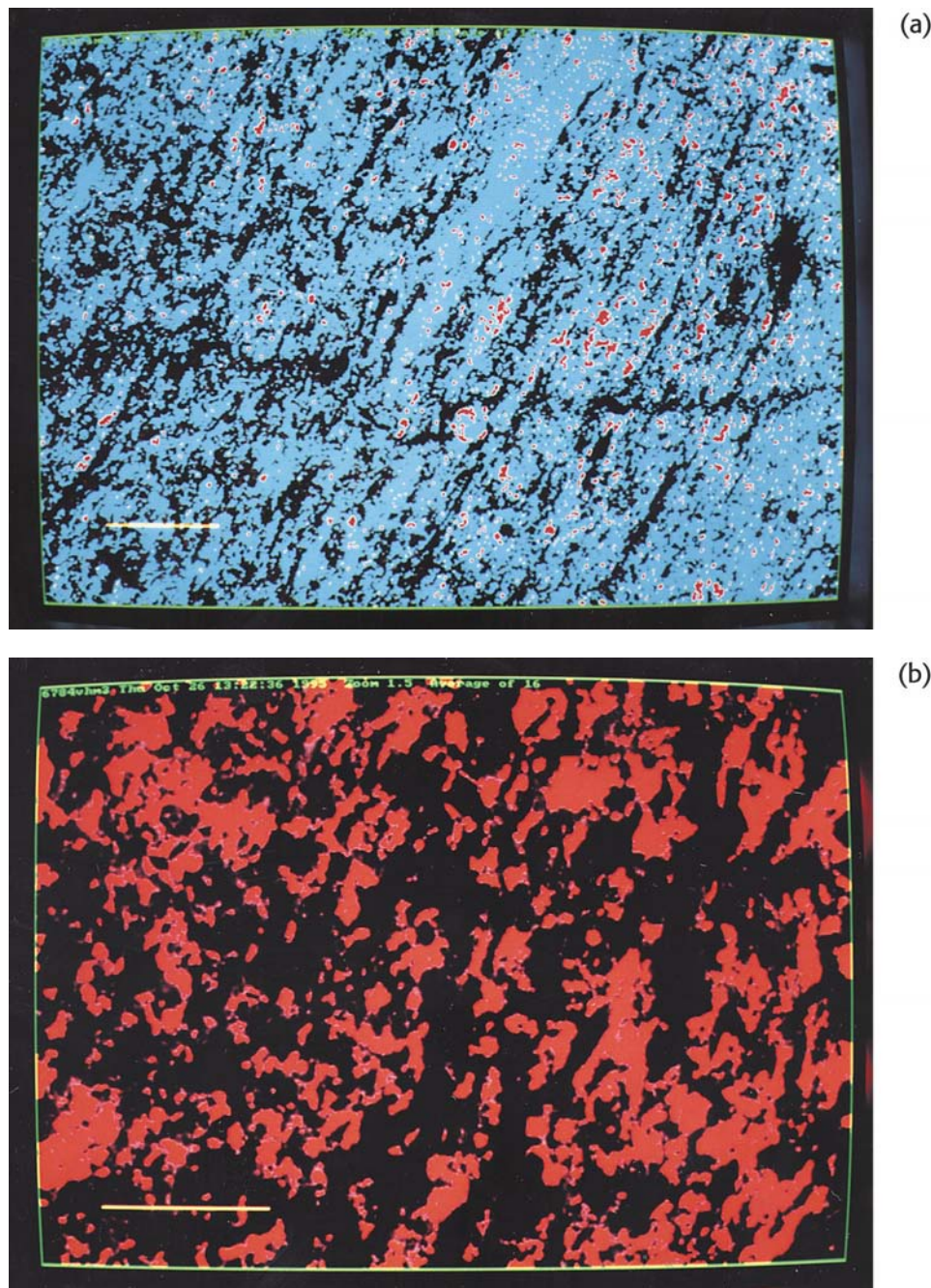
Vertical fractures are more common in less porous beds and laminae and typically terminate or change orientation at bedding planes. High-angle fractures interconnect microporous laminae (Figure 13). Microfractures are 0.1 to 0.01 mm wide and are present in most thin-section views of the porcelanite. Most vertical fractures have associated minor solution of matrix porcelanite, broken grains, and/or mineralization, indicating that the fractures are not drilling induced.

Matrix permeabilities from core analysis of porcelanites are typically low, averaging 0.8 md and ranging between 0.1 and 3 md. Regardless of the low permeability, much of the productivity of this interval is attributed to microfracturing of the porcelanite beds, although a classic dual-porosity system is not clearly documented from production tests. However, measured permeabilities may be somewhat biased, because

**Figure 10.** Scanning electron microscopy of porcelanite from well 313-30R (29R AB unit). (a) At a sample depth of 5937.75 ft (1809 m), clusters of quartz crystals 1 to 2  $\mu\text{m}$  in diameter are uniform in size. Microporosity is high, although pores are less than 2  $\mu\text{m}$  in diameter. Scale bar at lower right is 5  $\mu\text{m}$ . (b) A high magnification view of porous porcelanite from 6106.2 ft (1861 m) showing a preponderance of quartz in rounded clusters 1 to 5  $\mu\text{m}$  in diameter and pores generally less than 1  $\mu\text{m}$  in diameter. Scale bar at lower right is 0.5  $\mu\text{m}$ .



**Figure 11.** Confocal microscopy images from high-detritus porcelanite at 6784.0 ft (2067 m) in well 315X-31S (31S D unit). (a) At low magnification, nonporous matrix (black) is finely laminated with porcelanite (mixed matrix and porosity; blue). Scattered macroporosity (red) may represent molds of fossil fragments. A healed fracture (black) is present in center of image. Scale at lower left is 250  $\mu\text{m}$ . (b) At high magnification, nonporous matrix prevails (black), having pores disconnected and isolated (red). Scale at lower left is 25  $\mu\text{m}$ . Calculated porosity of sample is 14%.



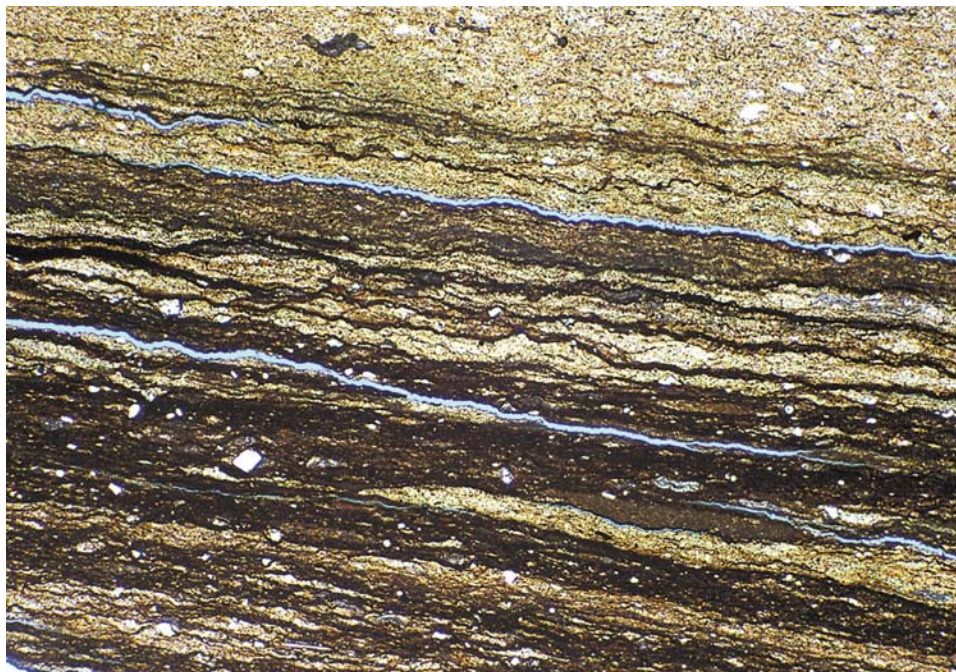
only the more cohesive samples can be analyzed, and much of the laminated porcelanite core is broken along bedding planes.

## LOG RESPONSE

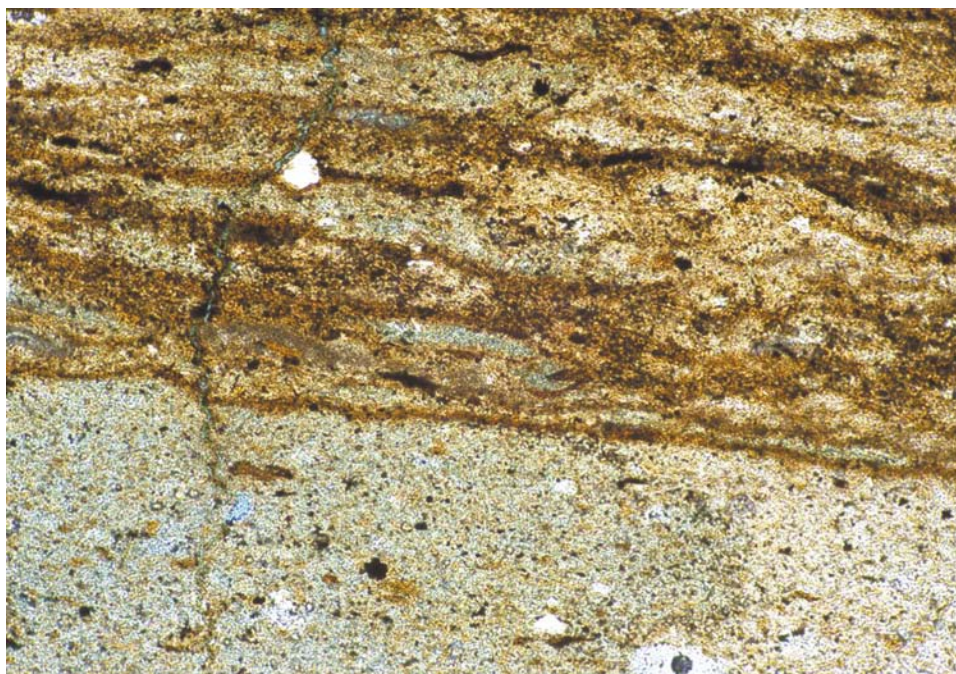
Quartz-phase porcelanites have a consistent log response (Figure 5). Gamma-ray response is low, and spontaneous potential (SP) is 30–55 mV from the clay

baseline. Deep resistivity averages 7 ohm m and can be greater in the D interval. Neutron porosity is 20–30% and separation between neutron porosity and bulk density curves is less than 3 porosity units, similar to that of a moderately clean sandstone. Alternating bands of high-resistivity porcelanite and sharply contrasting low-resistivity siliceous shale and organic-rich layers between 0.2 and 5 cm (0.1 and 2.0 in.) thick are identified by formation microimaging tools, as are larger scale fractures.





**Figure 12.** Photomicrograph of silty porcelanite having abundant dark organic-rich and clay-rich laminations from 6724.15 ft (2049 m) in well 315X-31S. Numerous partings are shown by blue dye and occur between porcelanite and organic-rich laminae. No evidence of mineralization is present on these fractures, and they may be drilling-induced or a result of the thin section preparation process. Alternatively, fractures such as these, if open in the reservoir, may contribute to the productivity observed from well tests. Diameter of the photomicrograph is 4.0 mm.



**Figure 13.** Photomicrograph of porous silty porcelanite (bottom) and laminated organic-rich high-detritus porcelanite (top) from 6724.15 ft (2049 m) in well 315X-31S. An open vertical fracture is present on the left of the image and connects porous porcelanite laminations. Evidence that minor fractures are open includes lining by petroleum and slight offset of laminations. Diameter of photomicrograph is 1.0 mm.

Porcelanites having higher opal-CT-phase content (22–35 wt. %) also have a distinctive log character. They have moderate SP and a lower deflection from the shale baseline than quartz-phase rocks, inverted resistivities averaging 5 ohm m, 35% average porosity values from neutron logs, and slight to moderate po-

rosity log crossover effect due to their low densities. Similar log responses in opal-CT porcelanite are present in the Antelope Shale Member at the Lost Hills field (McGuire et al., 1983) (Figure 5).

Siliceous shale and clay shale are easily distinguished from reservoir porcelanites on logs. They

exhibit low to moderate SP, low resistivity (2.5 to 4 ohm m), and a more argillaceous neutron-density log response.

## DISCUSSION

### Fractures as a Factor in Reservoir Architecture

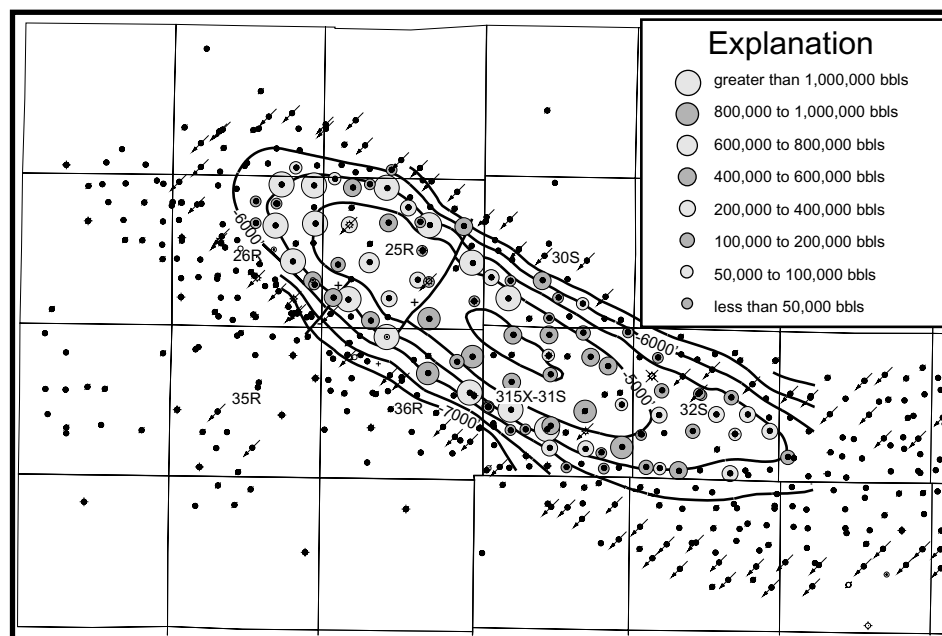
Fractures are significant in the reservoir architecture for the porcelanite reservoirs. However, compared to other quartz-phase Monterey reservoirs described from the coastal basins (for instance, Narr [1991]), the Elk Hills porcelanites have a relatively low density of large fractures.

Natural fractures help deliver hydrocarbons from the tight matrix to wellbores. Based on production responses, many of the fractures must be open to produce the high fluid volumes seen in many wells. Larger vertical fractures (those noted on the imaging logs) are believed to be the most permeable, which is consistent with observations by MacKinnon (1989) for the Santa Barbara area. Initially oil-bearing, most large fractures now produce water. The high water production generally suppresses oil production and results in less profitable wells. Successful exploitation of the tight porcelanite matrix has been accomplished by avoiding intervals bearing these larger fractures in new well completion programs.

Recently completed wells that avoided the larger fractures have production responses that indicate that the smaller scale fractures are a major factor in accessing the porcelanite matrix. Well 315X-31S was completed in 1996 in intervals containing the inferred bedding fractures, as well as microfractures, but few larger fractures. Production rates are higher than would be expected from the tight porcelanite matrix and from small vertical fractures alone. Based on core and formation microimaging logs, there are not enough high-angle fractures present in the completed interval to match the production response. Production from open bedding-plane fractures may provide the additional interval permeability to explain observed production rates. Initial production (after acid stimulation) from 122 ft of perforations was 300 BOPD; cumulative production through June of 1998 is 134,000 bbl of oil.

Production trends on the 31S anticline further support the presence of locally abundant open bedding-plane fractures (Figure 14). Wells having the highest cumulative oil production are located on the flanks of the anticline in areas of highest formation dip (40–70°). Wells having the lowest cumulative oil rates are on the noses of the structures, where dip is less than 30°. Although the fold nose contains the maximum bending, and should be the most intensely fractured, bedding-plane fractures are not open because of overburden stress. However, on the flanks of the structure in areas of high dip, bedding-plane fractures are influenced

**Figure 14.** Bubble map of oil production from the 31S D unit. Higher production occurs on the flanks of the anticline, a result of a strong gravity drainage mechanism that may be aided by open bedding-plane fractures. Production is significantly lower on the gently plunging east nose, where bedding-plane fractures may be closed. Crestal production is low to minimize gas production.



more by the horizontal stresses (which are much less than the overburden stress) and can remain open in reservoir conditions. Gravity drainage assists oil as it moves downslope along bedding to wellbores, contributing to high cumulative oil production.

As described by Dholakia et al. (1998), fractures in the Monterey of the western San Joaquin basin may have formed during anticlinal growth. Concentric folding creates planes of slip between beds; slip is greatest on the fold limbs. Increased slip on the limbs of bedding-plane faults leads to fracturing perpendicular to bedding. Higher levels of slip, as seen in outcrop at Chico Martinez Creek (Figure 1) (Dholakia et al., 1998) result in brecciation of bedding. Dholakia et al.'s model seems appropriate for the Elk Hills porcelanite section. Folding on the limbs of the large 31S anticline created fractures between beds of varying porcelanite and organic material content. On the more tightly folded 29R structure, slip along bedding fractures led to the development of more intense bed-perpendicular fracturing, which is consistent with Dholakia et al.'s fracture model. Nowhere at Elk Hills is folding so severe as to create zones of brecciation (at least not in cored intervals).

### Preservation of Microporosity

The diagenetic process of altering diatomite to quartz-phase porcelanite is typically accomplished by the reprecipitation of silica into nearby pores (Williams et al., 1985) and by the collapse of the crystalline framework due to the loss of strength during dissolution (Isaacs, 1981b). The release of water from opal-A and opal-CT dissolution and from compaction may lead to increased pore pressures and fracture formation, and silica-laden waters may move upsection to complete opal-CT or quartz precipitation in the remaining porosity (Eichhubl and Boles, 1998).

To preserve the higher porosity observed in Elk Hills porcelanites, the matrix must not fully collapse during the diagenetic process nor silica reprecipitate to fill the matrix porosity. Williams et al. (1985) and Chaika (1998) suggest a process in which silica remains in the host rock but not as opal-CT or quartz. By combining with other available elements, clay minerals or zeolites may form in preference to opal-CT or quartz. This process may occur in the Elk Hills porcelanites, but not enough clay is identified by x-ray diffraction analysis to account for the amount of silica released in the diagenetic process, although an unknown volume of clay may have precipitated at crystal sizes too small

for x-ray diffraction to detect. Alternatively, at Elk Hills we propose that silica reforms as quartz but crudely mimics the former opal-CT structure (as pseudomorphs) (Williams et al., 1985) to preserve the higher matrix porosity through the following four steps:

1. A normal transition occurs from opal-A to opal-CT, having local formation of opal-CT that partially fills matrix porosity, lowering the porosity from 50% or greater to an average of 33%. Limited fracturing occurs, possibly due to the initial folding of the structures or through minor breaks formed during compaction.
2. Structural growth continues to nearly the extent present today, forming the closures necessary to trap oil and gas. Fractures are created, including the bedding-plane fractures, small fractures, and larger faults such as the 26R fault.
3. Petroleum is generated in the deeper Buttonwillow and Maricopa subbasin areas located north and south of Elk Hills (Figure 1) (Ziegler and Spotts, 1978). Migration occurs into the Elk Hills traps, prior to onset of the opal-CT-quartz transformation. Petroleum enters the opal-CT-phase reservoirs through the bedding-plane fractures, small fractures, and larger faults, displacing the connate water in the opal-CT porcelanite matrix.
4. With additional burial, the opal-CT-quartz transformation begins. The presence of hydrocarbons in pores restricts the movement of silica-rich waters to the immediate vicinity of the opal-CT lepispheres. Replacement of opal-CT occurs at an extremely local scale, having reprecipitating quartz forming a crude pseudomorph of the opal-CT framework (as in Williams [1982] and Williams et al., [1985]) (Figure 10). The former opal-CT porosity does not fill with precipitating quartz because much of the pore space is already filled with hydrocarbons. Because further quartz precipitation is prevented, silica-rich water that forms from the release of caged water within the cristobalite mineral framework (Hurd and Theyer, 1977) and from compaction (Murata and Larson, 1975) adds to the pore pressure. Higher pore pressures activate the existing fault and fracture system, and excess fluid enters the fractures to seek intervals of lower pressure. Because oil already occupies the available porosity, and because water is denser than oil, water produced from the final phase change to quartz moves in preference downslope on the bedding fractures.



Some opal-CT is present at the crest of the 29R structure, indicating that the transformation was interrupted by the Pleistocene uplift of the Elk Hills structure.

The presence of chert cement in the 26R sandstone in areas near the 26R fault indicates that the fault may have been a conduit to move silica-rich water from the overpressured 31S D porcelanite to the less pressured 26R reservoir (Figure 3). The water would need to move about 300 m (1000 ft) south along the fault to reach the 26R reservoir. Microcrystalline quartz cement occurs locally below the oil-water contact in the 26R sandstone (J. Boles, 1998, personal communication), indicating that the formation of the chert cement occurred after migration of petroleum into the 26R reservoir trap.

## SUMMARY

The most productive intervals of the Elk Hills 29R AB and 31S D reservoirs contain one principle rock type: low-detritus porcelanite derived primarily from diatom debris. Throughout most of California, diagenetic processes alter the diatoms to hard, brittle, low-porosity chert and porcelanite. However, in the central San Joaquin basin, quartz-phase porcelanite is porous, laminated, and rich in organic material. The origin of this variation of porcelanite is attributed to (1) migration of petroleum into the reservoirs while the matrix was in opal-CT phase, (2) preservation of an open matrix as quartz replaced opal-CT in the immediate vicinity of opal-CT lepispheres (possibly as a pseudomorph of opal-CT mineral structure), and (3) petroleum-filled pores preventing the migration and precipitation of additional silica that could fill porosity. Large fractures are present in the reservoirs but not nearly to the extent observed in other California oil fields. Microfractures are present throughout the porcelanite intervals. Fractures occur parallel with bedding and perpendicular to bedding. Bedding-plane fractures are probably open along the limbs of the Elk Hills anticlines. Overburden pressure probably keeps bedding-plane fractures closed on the less productive, low dip nose area of the reservoirs. High-angle fractures provide only moderate vertical communication.

The oil-saturated microporous matrix provides most of the oil storage for the 29R AB and 31S D reservoirs, and fractures primarily at smaller scales form the delivery system for the porcelanite. On the steeper

flanks of the anticlines, oil moves from the matrix into bedding-plane fractures, and downslope under gravity flow. The ranges of matrix and fracture permeabilities probably overlap, which masks the identification of classic dual porosity reservoir responses. Oil moves slowly from the matrix because of the extremely small pore throats that average 1  $\mu\text{m}$  in diameter. However, gas can move through these small throats and the smallest fractures, resulting in an extraordinarily large gas recovery. Because the porcelanite has a significant organic component, desorbed gas is also a significant source of methane in the reservoir (McIntyre et al., 1997). Gas production should continue as the reservoir pressure declines and gas is released from organic material, as well as from the liquid confined to the lowest permeable recesses of the matrix.

Porous quartz-phase porcelanite represents another productive variation of the diverse reservoir types of the Monterey Formation. We suspect additional porcelanite reservoirs in the southwest San Joaquin basin contain similar porosity trends as Elk Hills because of the common geologic history of the area. Other basins of California may also contain porous quartz-phase porcelanites, provided that oil migration occurs before the transition from opal-CT to quartz.

## REFERENCES CITED

- Bandy, O. L., and R. E. Arnal, 1969, Middle Tertiary basin development, San Joaquin Valley, California: Geological Society of American Bulletin, v. 80, p. 783–819.
- Bramlette, M. N., 1946, The Monterey Formation of California and the origin of its siliceous rocks: U.S. Geological Survey Professional Paper 212, 57 p.
- California Division of Oil and Gas, 1998, 1997 annual report of the State Oil and Gas Supervisor: Sacramento, California, California Department of Conservation publication no. PR06, 267 p.
- Castillo, D. A., and M. D. Zoback, 1994, Systematic variations in stress state in the southern San Joaquin Valley: inferences based on well-bore data and contemporary seismicity: AAPG Bulletin, v. 78, p. 1257–1275.
- Chaika, C. J., 1998, Porosity reduction during silica diagenesis, in C. J. Chaika, Physical properties and silica diagenesis: Ph.D. thesis, Stanford University, Stanford, California, p. 1–21.
- Dholakia, S. K., A. Aydin, D. D. Pollard, and M. D. Zoback, 1998, Fault-controlled hydrocarbon pathways in the Monterey Formation, California: AAPG Bulletin, v. 82, p. 1551–1574.
- Dunwoody, J. A., 1986, Correlation section no. 8 (revised) across southern San Joaquin Valley from San Andreas fault to Sierra Nevada foothills: Pacific Section AAPG, cross section CS8R.
- Eichhubl, P., and R. J. Behl, 1998, Diagenesis, deformation, and fluid flow in the Miocene Monterey Formation, in P. Eichhubl, ed., Diagenesis, deformation, and fluid flow in the Miocene Monterey Formation: Pacific Section SEPM, book 83, p. 5–13.
- Eichhubl, P., and J. R. Boles, 1998, Vein formation in relation to burial diagenesis in the Miocene Monterey Formation, Arroyo

- Burro Beach, Santa Barbara, California, in P. Eichhubl, ed., Diagenesis, deformation, and fluid flow in the Miocene Monterey Formation: Pacific Section SEPM, book 83, p. 15–36.
- Fredrich, J. T., K. H. Greaves, and J. W. Martin, 1993, Pore geometry and transport properties of Fontainebleau sandstone: International Journal of Rock Mechanics, Mineral Science and Geomechanical Abstracts, v. 30, p. 691–697.
- Graham, S. A., 1978, Role of Salinian block in evolution of San Andreas fault system, California: AAPG Bulletin, v. 62, p. 2214–2231.
- Graham, S. A., and L. A. Williams, 1985, Tectonic, depositional, and diagenetic history of Monterey Formation (Miocene), central San Joaquin basin, California: AAPG Bulletin, v. 69, p. 365–411.
- Graham, S. A., L. A. Williams, M. Bate, and L. S. Weber, 1982, Stratigraphic and depositional framework of the Monterey Formation and associated coarse clastics of the central San Joaquin basin, in L. A. Williams and S. A. Graham, eds., Monterey Formation and associated coarse clastic rocks, central San Joaquin basin, California: Pacific Section SEPM, Annual Field Trip Guidebook, p. 3–16.
- Graham, S. A., R. G. Stanley, J. V. Bent, and J. B. Carter, 1989, Oligocene and Miocene paleogeography of central California and displacement along the San Andreas fault: Geological Society of America Bulletin, v. 101, p. 711–730.
- Grimm, K. A., and D. L. Orange, 1997, Synsedimentary fracturing, fluid migration, and subaqueous mass wasting: intrastratal microfractured zones in laminated diatomaceous sediments, Miocene Monterey Formation, California: Journal of Sedimentary Research, v. 67, p. 601–613.
- Harding, T. P., 1976, Tectonic significance and hydrocarbon trapping consequences of sequential folding synchronous with San Andreas faulting, California: AAPG Bulletin, v. 60, p. 356–378.
- Hurd, D. C., and F. Theyer, 1977, Changes in the physical and chemical properties of biogenic silica from the central equatorial Pacific: part II: refractive index, density, and water content of acid-cleaned samples: American Journal of Science, v. 277, p. 1168–1202.
- Isaacs, C. M., 1981a, Outline of diagenesis in the Monterey Formation examined laterally along the Santa Barbara coast, California, in C. M. Isaacs, ed., Guide to the Monterey Formation in the California coastal area, Ventura to San Luis Obispo: Pacific Section AAPG, v. 52, p. 25–38.
- Isaacs, C. M., 1981b, Porosity reduction during diagenesis of the Monterey Formation, Santa Barbara coastal area, California, in R. E. Garrison and R. G. Douglas, eds., The Monterey Formation and related siliceous rocks of California: Pacific Section SEPM, p. 257–271.
- Isaacs, C. M., 1981c, Field characterization of rocks in the Monterey Formation along the coast near Santa Barbara, California, in C. M. Isaacs, ed., Guide to the Monterey Formation in the California coastal area, Ventura to San Luis Obispo: Pacific Section AAPG, v. 52, p. 39–53.
- MacKinnon, T. C., 1989, Petroleum geology of the Monterey Formation in the Santa Maria and Santa Barbara coastal and offshore areas, in T. MacKinnon, ed., Oil in the California Monterey Formation: Washington, D.C., American Geophysical Union, Field Trip Guidebook T311, p. 11–27.
- MacPherson, B. A., 1978, Sedimentation and trapping mechanism in upper Miocene Stevens and older turbidite fans of southeastern San Joaquin Valley, California: AAPG Bulletin, v. 62, p. 2243–2278.
- Maher, J. C., R. D. Carter, and R. J. Lantz, 1975, Petroleum geology of naval petroleum reserve No. 1, Elk Hills, Kern County, California: U.S. Geological Survey Professional Paper 912, 109 p.
- McGuire, M. D., J. R. Bowersox, and L. J. Earnest, 1983, Diagenetically enhanced entrapment of hydrocarbons—southeastern Lost Hills fractured shale pool, Kern County, California, in C. M. Isaacs and R. E. Garrison, eds., Petroleum generation and occurrence in the Miocene Monterey Formation, California: Pacific Section SEPM, p. 171–183.
- McIntyre, J. L., T. J. Hampton, S. A. Reid, M. L. Wilson, T. W. Thompson, and K. H. Greaves, 1997, Preliminary quantification of adsorbed gas in Monterey Shale reservoirs at Elk Hills, Kern County, California (abs.): AAPG Bulletin, v. 81, p. 690.
- Murata, K. J., and R. R. Larson, 1975, Diagenesis of Miocene siliceous shales, Temblor Range, California: U.S. Geological Survey Journal of Research, v. 3, no. 5, p. 553–566.
- Narr, W., 1991, Fracture density in the deep subsurface: techniques with application to Point Arguello oil field: AAPG Bulletin, v. 75, no. 8, p. 1300–1323.
- Reid, S. A., 1990, Trapping characteristics of upper Miocene turbidite deposits, Elk Hills field, Kern County, California, in J. G. Kuespert and S. A. Reid, eds., Structure, stratigraphy and hydrocarbon occurrences of the San Joaquin basin, California: Pacific Section AAPG, guidebook GB65, p. 141–156.
- Reid, S. A., 1995, Miocene and Pliocene depositional systems of the southern San Joaquin basin and formation of sandstone reservoirs in the Elk Hills area, California, in A. E. Fritsche, ed., Cenozoic paleogeography of the western United States-II: Pacific Section SEPM, book 75, p. 131–150.
- Reid, S. A., and M. L. Wilson, 1990, Field trip stops at the Elk Hills oil field, in J. G. Kuespert and S. A. Reid, eds., Structure, stratigraphy and hydrocarbon occurrences of the San Joaquin basin, California: Pacific Section AAPG, guidebook GB65, p. 319–329.
- Ruessink, B. H., and D. G. Harville, 1992, Quantitative analysis of bulk mineralogy: the applicability and performance of XRD and FTIR: Society of Petroleum Engineers International Symposium on Formation Damage Control, SPE 23828, p. 533–546.
- Shimmield, G. B., and N. B. Price, 1984, Recent dolomite in hemipelagic sediments off Baja California, in R. E. Garrison, M. Kastner, and D. H. Zenger, eds., Dolomites of the Monterey Formation and other organic-rich units: Pacific Section SEPM, v. 41, p. 5–18.
- U.S. Department of Energy, 1997a, Stevens 29R/24Z Shale, in Opportunities at Elk Hills: Washington, D.C., U.S. Department of Energy, v. 6, chapter 12, 32 p.
- U.S. Department of Energy, 1997b, Stevens 31S CD Shale, in Opportunities at Elk Hills: Washington, D.C., U.S. Department of Energy, v. 5, chapter 11, 26 p.
- Webb, G. W., 1981, Stevens and earlier Miocene turbidite sandstone, southern San Joaquin Valley, California: AAPG Bulletin, v. 65, p. 438–465.
- Williams, L. A., 1982, Lithology of the Monterey Formation (Miocene) in the San Joaquin Valley of California, in L. A. Williams and S. A. Graham, eds., Monterey Formation and associated coarse clastic rocks, central San Joaquin basin, California: Pacific Section SEPM, p. 17–35.
- Williams, L. A., G. A. Parks, and D. A. Crerar, 1985, Silica diagenesis, I: solubility controls: Journal of Sedimentary Petrology, v. 55, p. 301–311.
- Wilson, M. L., R. E. Dorsey, and M. Allan, 1997, Geology and production implications of debris flows in the C & D shale reservoirs, Elk Hills giant oil field, California (abs.): AAPG Bulletin, v. 81, p. 694.
- Ziegler, D. L., and J. H. Spotts, 1978, Reservoir and source-bed history of Great Valley, California: AAPG Bulletin, v. 62, p. 813–826.